International Journal of Mechanical Sciences 214 (2022) 106887

Contents lists available at ScienceDirect

International Journal of Mechanical Sciences

journal homepage: www.elsevier.com/locate/ijmecsci

Closed-form dynamic stiffness formulation for exact modal analysis of tapered and functionally graded beams and their assemblies

Xiang Liu [a,b,c], Le Chang [a,b,c], J. Ranjan Banerjee [d], Han-Cheng Dan [b,e,*]

[a] Key Laboratory of Traffic Safety on Track, Ministry of Education, School of Traffic & Transportation Engineering, Central South University, Changsha, China
[b] Joint International Research Laboratory of Key Technology for Rail Traffic Safety, Central South University, Changsha, China
[c] National & Local Joint Engineering Research Center of Safety Technology for Rail Vehicle, Central South University, Changsha, China
[d] School of Mathematics, Computer Science and Engineering, City University London, London EC1V 0HB, UK
[e] School of Civil Engineering, Central South University, Changsha, China

ARTICLE INFO

Keywords:
Tapered beams
Functionally graded beams
Dynamic stiffness method
Wittrick-Williams algorithm
Free vibration analysis

ABSTRACT

The paper proposes a closed-form dynamic stiffness (DS) formulation for exact transverse free vibration analysis of tapered and/or functionally graded beams based on Euler–Bernoulli theory. The novelties lie in both the DS formulation and the solution technique. For the formulation, the developed DS is applicable to a wide range of non-uniform beams whose bending stiffness and linear density are assumed to be polynomial functions of position. This fills a gap of existing closed-form DS element library which is generally limited to linearly tapered/functionally graded beams. For the solution technique, an elegant and efficient J_0 count of tapered element is proposed to apply the Wittrick-Williams (WW) algorithm most effectively. The investigation sheds lights on the so-called J_0 count challenge of the algorithm for other DS elements. The above two novelties make exact and highly efficient modal analysis possible for a wide range of tapered and/or functionally graded beams, without resorting to series solution, numerical integrations or refined mesh discretization. Results for a particular case show excellent agreement with published results. Moreover, we investigate the effects of the taper/functional gradient rate/index and boundary conditions on the free vibration behaviour. Benchmark solutions are provided for individual beams as well as beam assemblies.

1. Introduction

Beam structures are commonly used as load bearing structures in many engineering fields such as civil, aeronautical, mechanical and electronic engineering. Such structures are often optimized to improve the vibration and noise properties. For example, a tapered or functionally graded beam can be adopted for a light-weight design or specific wave propagation effects, such as acoustic black hole effect [1], wave propagation control [2], piezoelectric energy harvesting [3] amongst many others including architectural considerations.

Of course, in order to design tapered beams, the finite element method (FEM) is probably the most commonly used method in engineering. When modelling such beams with continuously varying cross-section or material, the FEM approximates the continuous beams by the so called finite elements. The shape functions for each element are assumed to be approximate polynomials, leading to separate and frequency-independent element mass and stiffness matrices. Finally the elemental matrices are assembled in the FEM resulting in global stiffness and mass matrices with frequency as the eigenvalue parameters in free vibration problem. This becomes a generalised eigenvalue problem which can be computed by usual linear algebra solvers. Based on the uniform Bernoulli–Euler theory and the Timoshenko theory respectively, Shahba et al. [4,5] derived arbitrarily tapered or axially functionally graded beam elements and investigated their stability and free vibration characteristics. Both free vibration and wave propagation analysis of rotating Euler–Bernoulli tapered beams were also reported [6] by using spectrally formulated finite elements. Ramalingerswara and Ganesan [7] investigated the harmonic response of composite tapered beams by using FEM and a higher order shear deformation theory based on a similar principle of higher order plate theory. However, due to both the discretization of continuous function and the approximation of the shape functions, only the lower order eigenvalues could be accurately extracted from the FEM model. If one needs more accurate results especially in the high frequency range, a much finer mesh will be required, particularly for a tapered or functionally graded beam than that for a uniform beam.

Meanwhile, analytical methods can serve as useful alternatives whose advantages include accuracy, efficiency, convenience and

* Corresponding author at: School of Civil Engineering, Central South University, Changsha, China.
E-mail address: danhangcheng@csu.edu.cn (H.-C. Dan).

https://doi.org/10.1016/j.ijmecsci.2021.106887
Received 29 July 2021; Received in revised form 14 October 2021; Accepted 19 October 2021
Available online 29 October 2021

physical-meaning clarity. For example, the Rayleigh–Ritz method is a common analytical method. By employing the Rayleigh–Ritz method, Abrate [8] performed the longitudinal vibration analysis of a variety of tapered rods with quadratic polynomials for the area along the length; Zhou and Cheung [9] established admissible functions representing the solution to analyse the free vibration of a type of rectangular tapered beams whereas the transverse vibration of rectangular Mindlin plates with variable thickness was investigated in [10]. On the other hand, the variational iteration method [11] was used to study the free vibration of a linearly tapered beam mounted on two-degrees of freedom spring-damper-mass subsystems. Huang and Lee [12] performed free vibration analysis of axially functionally graded beams with non-uniform cross-section based on the Bernoulli–Euler theory. The governing differential equation with variable coefficients was transformed into Fredholm integral equation, and the shape function was expanded in power series. Ashour [13] investigated the transverse vibration of orthotropic rectangular plates of variable thickness by combining the finite strip technique with the transfer matrix method. The asymmetric development method [14] was used for the free vibration of axially functionally graded beams based on the Bernoulli–Euler theory. The investigation in [14] obtained approximate analytical formulas for natural frequencies under several classical boundary conditions. Hein and Feklistova [15] studied the free vibration of non-uniform and axially functionally graded beams using the Haar wavelet approach and the Bernoulli–Euler theory. Based on the Rayleigh-Love theory, Banerjee et al. [16] analysed the axial vibration of a conical rod. By rewriting the governing differential equation into the Legendre's equation, the shape function was obtained in series form, and the natural frequencies were computed by the authors by substituting the boundary conditions to eliminate the unknown constants. By contrast, the transfer matrix method was employed by Mahmoud [17] to determine the natural frequencies of axially functionally graded tapered cantilever Bernoulli–Euler beams with point masses at the tips. However, all of the above analytical methods are based on approximate series-form of shape functions, leading to approximate results. There are, of course, other research based on exact general solutions for some particular tapered beams. For instance, the authors of [8] obtained the exact natural frequency solutions of classical bar with quadratic cross-section area and quartic cross-section area variations. Ece et al. [18] gave analytical solution for the free vibration of tapered beam with exponential cross-sectional area and moment of inertia variations. Jong-Shyong Wu [19] summarized the analytical solutions in the form of Bessel functions for a number of linearly tapered beams, including axial vibration of conical rods, torsional vibration of conical shafts and bending vibration of single-tapered beams. Zhao et al. [20] solved the analytical shape function of a parabolically tapered annular Euler beam by using method of substitution. Eventually, the natural frequencies and mode shapes were solved by them using the Galerkin method. By applying the coupled placement field method, Rajesh and Saheb [21] performed the large deflection free vibration analysis of linearly tapered Timoshenko beam and obtained closed form expression of frequency ratio for hinged-hinged and clamped-clamped boundary conditions. Banerjee and Ananthapuvirajah [22] utilized Bessel functions to represent the free vibrational shape function of linearly tapered Bernoulli–Euler beam accurately, and computed the natural frequencies by imposing the boundary conditions. However, the above methods can only be applied to a single tapered beam under special boundary conditions, and cannot be applied to an assembly or combination of tapered beams or for complicated boundary conditions in engineering.

Different from the above analytical methods, the dynamic stiffness (DS) method uses the frequency-dependent shape function to derive the dynamic stiffness matrix of a structural element, which can be assembled directly to model complex built-up structures and importantly, any boundary conditions can be easily imposed. The DS method was first proposed by Kolousek [23]. Since then, many investigations have been carried out for the DS formulation in the free vibration and buckling analysis of the bars, beams, plates, shells, membranes and their assemblies. Another landmark in the DS method is the development of the solution technique namely the Wittrick-Williams (WW) algorithm [24], which facilitates an efficient and accurate eigenvalue analysis based on the DS matrices. In what follows, we summarize the existing research from both DS formulation aspect as well as from the solution technique aspect.

As for the DS formulation aspect, there are a series of work on the DS formulation of tapered and/or functionally graded bars and beams, which can be classified into four broad category of methods:

Method 1 The first category of method is described to be as an approximate model of a tapered element using a number of uniform elements with different cross-section parameters, such as reported in [25,26]. By using this method, the natural frequencies and mode shapes of three types of linearly and parabolically tapered Bernoulli–Euler beams under axial force were computed and discussed in [25,26]. This method was implemented into a program called BUNVIS-RG [27] for the free vibration and buckling analyses of space frame structures consisting of tapered Timoshenko beams under axial force. Later, Banerjee [28] modelled tapered rotating Bernoulli–Euler beams as an assembly of a large number of uniform beams, where the DS matrix of a uniform rotating Bernoulli–Euler beam was derived by Frobenius method of power series solution. However, the disadvantage of this type of approach is that it requires a large number of elements and therefore reduces computational efficiency. Moreover, a numerical convergence test is needed to determine the natural frequencies with required accuracy.

Method 2 As proposed by Yuan et al. [29], the general solutions and their derivatives of non-uniform beams with gradual or stepwise cross-section can be numerically solved by ODE solvers, which are then used to formulate the DS matrices and the mesh generation rules of element length. Then the free vibration analysis of arbitrarily tapered or axial functionally graded beam based on Timoshenko theory was performed by Yuan et al. [29]. Although the method is capable of providing highly accurate results, the number of degrees of freedom used is quite large which decreases the computation efficiency. This type of method is essentially a combination of analytical and numerical methods due to the fact that the general solutions are computed by using the numerical ODE solvers.

Method 3 The DS formulations are developed in this method based on series form or approximate polynomial shape functions. For example, Banerjee et al. [30,31] used the Frobenius method to solve the differential equations and then established the dynamic stiffness matrix. Combined with the WW algorithm, natural frequencies of linearly tapered rotating Bernoulli–Euler beam [30] and Rayleigh-Love bar [31] were respectively computed by them. Leung and Zhou [32] applied the Frobenius method in the DS formulation of transverse vibration of tapered or axial functionally graded Timoshenko beams, to compute the natural frequencies. Similarly, Frobenius method was also used to formulate the transfer matrix [33] to analyse the free vibration of linearly tapered beam based on Bernoulli–Euler theory, and the natural frequencies were computed by the determinant of the transfer matrix. Kim et al. [34] adopted approximate polynomials as the shape function leading to the dynamic stiffness matrix, which was transformed into a state-vector form. However, it was found that in general, many series terms were required to converge upon results with acceptable accuracy.

Method 4 Dynamic stiffness formulation can also be achieved based on the closed-form exact solution of tapered beams, but this method is limited to the case when the governing differential

equation has closed-form exact general solution. Kolousek [23] first proposed the dynamic stiffness matrix of a linearly tapered beam based on the exact shape function in the form of Bessel functions. Later, Banerjee and his coauthors [35] formulated the explicit expressions of DS matrices for torsion, axial and transverse free vibration of linearly tapered beam, based on the closed-form Bessel equation. Su et al. [36] formulated the DS for a functionally graded Bernoulli–Euler beam with material parameters varying in power function along the thickness direction, and the natural frequencies and mode shapes were computed by applying the WW algorithm. The explicit expressions of the DS matrix missing in [36] was later provided by Banerjee and Ananthapuvirajah [37]. Recently, Popov [38] stated the transfer matrix can be developed without deriving the explicit exact general solution as in the DS formulation [37]. In another research, Banerjee et al. [16] developed the DS matrix of a linearly tapered Rayleigh-Love rod, and natural frequencies for both individual rods and their assemblies were computed. To get more details, [39] summarized the historical development of the DS method.

Therefore, it can be easily seen from the above that Method 4 being a closed-form exact formulation is the most efficient and accurate DS formulation for tapered beams among the four methods. Nevertheless, all existing research has been confined to linearly tapered beams so far [16,23,35,37]. Although nonlinear tapered beams are sometimes more commonly utilized in engineering applications, there appears to be no closed-form DS formulation available for it. A closed-form DS for tapered/functionally beams whose bending stiffness and linear density are assumed to be polynomial functions of position will no-doubt fill an important gap in the literature and add value to the closed-form DS element library of tapered/functionally graded beams with arbitrary cross sections.

Subsequently, once the analytically formulated matrices (such as dynamic stiffness matrix or transfer matrix) are developed, one needs to extract the natural frequencies and mode shapes from the analytically formulated matrices (based on either series-form solutions or closed-form solutions). There are generally two types of eigenvalue solution techniques available for this purpose.

Technique 1 One of the most commonly used eigenvalue solution technique is to determine the eigenvalue when the determinant of the system matrix becomes zero. This technique is used by most of the analytical methods (e.g., see [8,19,20]), including transfer matrix method [8,17,33,34,38,40]. However, the determinant method needs the evaluation of the determinant numerically for a frequency range. Deciding the step size to determine the zeros of the frequency-determinant and avoid the poles is problematic and far from being trivial. The problem arises because a small step size leads to unnecessary computational cost whereas a large step size increases the possibility of missing some genuine natural frequencies. This is especially true for complex structures and also when computing higher order natural frequencies. The problem is further compounded by the fact that the frequency determinant often involves complex and irregular transcendental functions such as the hyperbolic functions. Nevertheless, the potential pitfalls and drawbacks of the determinant method as mentioned above, still exist and hard to overcome.

Technique 2 The WW algorithm [41], which has been used in many DS formulations, e.g., [28,30,31,35–37,42]. The WW algorithm is probably the most suitable solution technique for dynamic stiffness models with the following advantages

(i) Accuracy: Eigenvalues within any required precision can be computed;
(ii) High efficiency: It is highly efficient mainly due to the small-size matrix;
(iii) Analytical elegance: Infinite eigenvalues can be extracted from the finite dimensional matrix;
(iv) Certainty: The algorithm ensures that no eigenvalue will be missed.

However, the advantages of (ii), (iii) and (iv) can be realized only when the key problem of the so called J_0 count (the mode count of all fully clamped members) in the WW algorithm can be effectively solved; Otherwise, either some spurious modes will enter into the calculation or some true modes will be missed, so that the advantage of the above (iv) certainty cannot be fully realised. Thus, J_0 count problem is an important key issue when applying the WW algorithm for the free vibration analysis. For the axial and transverse vibration of relatively simple uniform beam elements, the expression for J_0 count can be derived analytically, e.g., [39,41,43–50]. But for a tapered or functionally graded beam, the J_0 count problem becomes more challenging. We found that the only work that mentioned the J_0 problem of tapered beam is [35], which discussed the J_0 problem of linearly tapered beam. Most of the existing dynamic stiffness of tapered beams usually discretize a structure into elements small enough so that each element will have $J_0 = 0$ within the interested frequency range. However, as the number of elements is greatly increased, the above advantages of (ii) high efficiency and (iii) analytical elegance will be somehow sacrificed, let alone the fact that substructuring technique become less convenient to use for tapered beams compared to uniform beams. So it is very important to provide an efficient technique to compute the J_0 count of the tapered beam member for the WW algorithm to be most effective.

This paper essentially aims to fill the gap which is the limitation of the existing research that closed-form DS formulation is confined to linearly tapered and functionally graded beams only. The novelty of this paper is two fold: (1) A closed-form DS formulation of tapered and/or functionally graded beams is developed based on the exact general solution of the governing differential equation; (2) An efficient solution for the most crucial issue of J_0 count for the WW algorithm is proposed. By doing so, exact modal analysis can be efficiently performed for more general tapered and functionally graded beams and their assemblies. This undertaking is an important supplement to the existing non-uniform DS element library. A wide range of tapered and functionally graded beam members and their assemblies or when they are connected to uniform beams can be exactly modelled in the whole frequency range using a minimum number of degrees of freedom, and exact natural frequencies and mode shapes can be computed efficiently. This can be used for the efficient and accurate parametric studies and optimization of beam built-up structures.

The paper is organized as follows. Section 2 provides the development of DS formulation in explicit form based on the exact solution of tapered and/or functionally graded Euler–Bernoulli beam. Section 3 describes the modal analysis by using the WW algorithm, where the emphasis is placed on proposing an efficient and reliable J_0 count procedure for a tapered and/or functionally graded beam member. In Section 4, the proposed method is validated by comparing current solutions with published results and those computed by commercial FEM software, to demonstrate the exactness, efficiency and wide application scope of the proposed theory and solution technique. Finally, Section 5 concludes the paper.

2. Dynamic stiffness formulation

2.1. Governing differential equations and boundary conditions

The governing differential equation (GDE) for the flexural vibration of a tapered beam shown in Fig. 1 can be derived using Newton's law

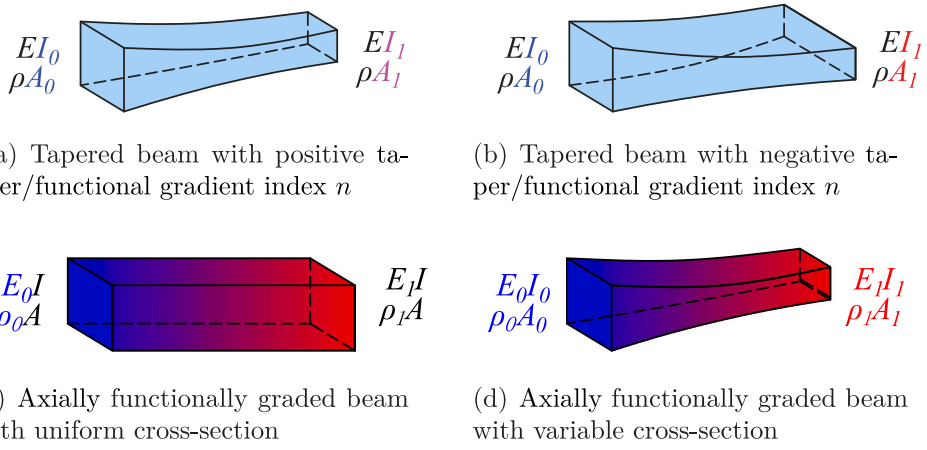

(a) Tapered beam with positive taper/functional gradient index n

(b) Tapered beam with negative taper/functional gradient index n

(c) Axially functionally graded beam with uniform cross-section

(d) Axially functionally graded beam with variable cross-section

Fig. 1. Several tapered and/or functionally graded beams developed in this paper.

or Hamilton's principle to give [33]

$$\frac{\partial^2}{\partial x^2}\left[E(x)I(x)\frac{\partial^2 w}{\partial x^2}\right] + \rho(x)A(x)\frac{\partial^2 w}{\partial t^2} = 0 \tag{1}$$

where

$$\rho(x)A(x) = \rho_0 A_0\left(1-\frac{c}{L}x\right)^n, \quad E(x)I(x) = E_0 I_0\left(1-\frac{c}{L}x\right)^{n+4} \tag{2}$$

where $w = w(x,t)$ is the flexural displacement, t is time, the flexural rigidity $E(x)I(x)$ and the mass of the beam per unit length $\rho(x)A(x)$ are functions of the spatial variable $x \in [0, L]$. Apparently, $E(x)I(x)$ depends on elasticity modulus $E(x)$ and the second moment of area $I(x)$ and $\rho(x)A(x)$ is decided by the mass density of beam material $\rho(x)$ and the cross-sectional area $A(x)$. Therefore, the closed-form DS formulation derived in this paper is applicable to tapered beams, functionally graded beams and functionally graded beams with variable cross-section as shown in Fig. 1, provided that the beam parameters meet the Eq. (2) requirements. For a functionally graded beam, both $I(x)$ and $A(x)$ are constants. For a tapered beam, $E(x)$ and $\rho(x)$ are constants.

Both E and ρ are related to only one parameter, that is, the material type of the beam, while A and I are determined by two parameters, namely the length and width of the beam. This means that, for tapered beams, different cross-section types can have the same bending stiffness and linear density. Table 1 shows some representative combinations of cross-sectional parameters of tapered beams that are covered by the proposed DS formulation. In Table 1, b and h are the width and depth of the rectangular section, d and r are the thickness and outer radius of the thin annular section of a thin walled cylinder, R_a is the radius of the circular section or the outer radius of the annular section, and r_a is the inner radius of the annular section. The second moment of area of the rectangular section is $I = bh^3/12$ and the corresponding area is $A = bh$, and $I = \pi d r^3$, $A = 2\pi d r$ for the thin annular section. L is the total length of the beam. The subscript '0' represents the section parameters (A_0, I_0, b_0, d_0, r_0, r_{a0}, R_{a0} and h_0) of the largest cross-section of the beam which is considered to be the origin. c and n are the taper/functional gradient rate and taper/functional gradient index respectively, where $c \in (0, 1)$ and n can have any real values. We found that for a circular or annular cross-section, since there is only radius being the parameter and Eq. (2) must be satisfied, n can only be 4. For a rectangular section or a thin annular section, h (or r) is always proportional to $(1 - cx/L)^2$, and b (or d) is proportional to $(1 - cx/L)^{n-2}$. Interestingly, for rectangular section or a thin annular section, n is also allowed to be a fraction, which will be applicable to a wide range of cross-sections. It should be noted that the model proposed in this paper is not directly applicable to arbitrarily non-uniform beams but is a valuable contribution to the analysis of generally tapered and/or functionally graded beams. It is well known that many existing researches have used linearly

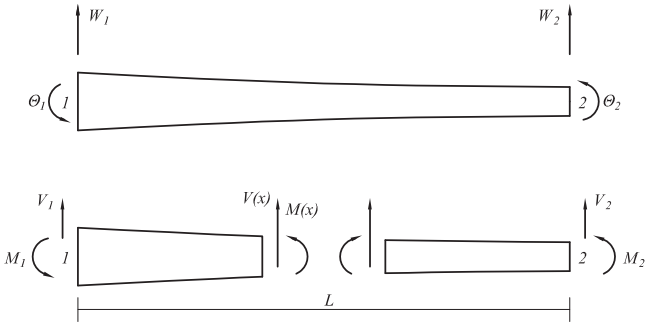

Fig. 2. Sign convention for a tapered Bernoulli–Euler beam element.

tapered and/or functionally graded elements (either dynamic stiffness elements [25,26] or transfer matrix elements [8,38]) to model higher-order beams, and consequently, a large number of linearly tapered and/or functionally graded elements are required to get results with acceptable accuracy. It is understandable that in order to approximate a higher-order function, a significantly fewer number of parabolic segments are required compared to the number of linear segments. Therefore, the higher-order tapered and/or functionally graded beam element proposed in this manuscript provide a more efficient yet more accurate tool to model tapered and/or functionally graded beam not covered in this paper, for instance, in the investigation of black holes.

We assume that the non-uniform beam is vibrating harmonically so that

$$w(x,t) = W(x)\mathrm{e}^{\mathrm{i}\omega t} \tag{3}$$

where $W(x)$ is the amplitude of the transverse displacement of the GDE in the frequency domain. Substituting Eq. (3) into Eq. (1), we get

$$E(x)I(x)\frac{\mathrm{d}^4 W}{\mathrm{d}x^4} + 2\frac{\mathrm{d}[E(x)I(x)]}{\mathrm{d}x}\frac{\mathrm{d}^3 W}{\mathrm{d}x^3} + \frac{\mathrm{d}^2[E(x)I(x)]}{\mathrm{d}x^2}\frac{\mathrm{d}^2 W}{\mathrm{d}x^2} - \rho(x)A(x)\omega^2 W = 0 \tag{4}$$

2.2. Exact general solutions

By introducing variable substitutions $\xi = x/L$, $\zeta = 1 - c\xi$ and $\eta = \ln\zeta$ [20], Eq. (4) becomes

$$\frac{\mathrm{d}^4 W}{\mathrm{d}\eta^4} + (2n+2)\frac{\mathrm{d}^3 W}{\mathrm{d}\eta^3} + \left(n^2+n-1\right)\frac{\mathrm{d}^2 W}{\mathrm{d}\eta^2} + \left(-n^2-3n-2\right)\frac{\mathrm{d}W}{\mathrm{d}\eta} - k_b^4 W = 0 \tag{5}$$

Table 1
Wide ranging possibilities covered by the non-uniform beam model developed in this work.

n	$I(x)/I_0$	$A(x)/A_0$	Rectangular/thin annular		Circular/annular	
			$b(x)/b_0$ $d(x)/d_0$	$h(x)/h_0$ $r(x)/r_0$	$R_a(x)/R_{a0}$	$r_a(x)/r_{a0}$
n	$(1-cx/L)^{n+4}$	$(1-cx/L)^n$	$(1-cx/L)^{n-2}$		–	–
4	$(1-cx/L)^8$	$(1-cx/L)^4$	$(1-cx/L)^2$		$(1-cx/L)^2$	$(1-cx/L)^2$
2	$(1-cx/L)^6$	$(1-cx/L)^2$	$(1-cx/L)^0$	$(1-cx/L)^2$		
1/3	$(1-cx/L)^{13/3}$	$(1-cx/L)^{1/3}$	$(1-cx/L)^{-5/3}$		–	–
0	$(1-cx/L)^4$	$(1-cx/L)^0$	$(1-cx/L)^{-2}$			
−2	$(1-cx/L)^2$	$(1-cx/L)^{-2}$	$(1-cx/L)^{-4}$			

where

$$k_b^4 = \rho_0 A_0 L^4 \omega^2 / E_0 I_0 c^4 \tag{6}$$

The auxiliary or characteristic equation of Eq. (5) is

$$r^4 + (2n+2)r^3 + \left(n^2+n-1\right)r^2 + \left(-n^2-3n-2\right)r - k_b^4 = 0 \tag{7}$$

which can be rewritten in the following form

$$\left[\left(r+\frac{n+1}{2}\right)^2 - \frac{n^2}{4} - n - \frac{5}{4}\right]^2 = k_b^4 + \left(\frac{n}{2}+1\right)^2 \tag{8}$$

with four roots

$$r_{1,2} = -\Gamma_1 \pm \sqrt{\Gamma_2 + \sqrt{\Gamma_3}}, \quad r_{3,4} = -\Gamma_1 \pm \sqrt{\Gamma_2 - \sqrt{\Gamma_3}} \tag{9}$$

where

$$\Gamma_1 = \frac{n+1}{2}, \quad \Gamma_2 = \frac{n^2}{4} + n + \frac{5}{4}, \quad \Gamma_3 = k_b^4 + \left(\frac{n}{2}+1\right)^2 \tag{10}$$

Thus the general solution of Eq. (5) can be written as

$$W(\eta) = \mathrm{e}^{-\left(\frac{n+1}{2}\right)\eta}\left[C_1\cos(k_1\eta) + C_2\sin(k_1\eta) + C_3\cosh(k_2\eta) + C_4\sinh(k_2\eta)\right] \tag{11}$$

where $C_1 - C_4$ are unknown constants.

In terms of the original spatial variable x, the solution given by Eq. (11) becomes

$$W(x) = \left(1-c\frac{x}{L}\right)^{-\frac{n+1}{2}}\left[C_1\cos\left(k_1\ln\left(1-c\frac{x}{L}\right)\right) + C_2\sin\left(k_1\ln\left(1-c\frac{x}{L}\right)\right) + C_3\cosh\left(k_2\ln\left(1-c\frac{x}{L}\right)\right) + C_4\sinh\left(k_2\ln\left(1-c\frac{x}{L}\right)\right)\right] \tag{12}$$

where

$$k_1 = \sqrt{-\Gamma_2 + \sqrt{\Gamma_3}}, \quad k_2 = \sqrt{\Gamma_2 + \sqrt{\Gamma_3}} \tag{13}$$

The amplitudes of the shear force (V) and bending moment (M) in the frequency domain take the following form

$$M(x) = EI(x)\frac{\mathrm{d}^2 W}{\mathrm{d}x^2} \tag{14}$$

$$V(x) = -\frac{\mathrm{d}}{\mathrm{d}x}\left(EI(x)\frac{\mathrm{d}^2 W}{\mathrm{d}x^2}\right) \tag{15}$$

Referring to Fig. 2, the displacement and force boundary conditions for the two nodes (1 and 2) of the beam element can be applied as follows

$$\begin{aligned} W_1 &= W(0), \quad \Theta_1 = \Theta(0), \quad M_1 = -M(0), \quad V_1 = -V(0) \\ W_2 &= W(L), \quad \Theta_2 = \Theta(L), \quad M_2 = M(L), \quad V_2 = V(L) \end{aligned} \tag{16}$$

Substituting Eqs. (12), (14) and (15) into Eqs. (16), we have

$$\mathbf{d} = \mathbf{D}\bar{\mathbf{c}}, \quad \mathbf{f} = \mathbf{F}\bar{\mathbf{c}} \tag{17}$$

with

$$\mathbf{d} = \begin{bmatrix} W_1 \\ \Theta_1 \\ W_2 \\ \Theta_2 \end{bmatrix} \quad \mathbf{f} = \begin{bmatrix} V_1 \\ M_1 \\ V_2 \\ M_2 \end{bmatrix} \quad \bar{\mathbf{c}} = \begin{bmatrix} C_1 \\ C_2 \\ C_3 \\ C_4 \end{bmatrix} \tag{18}$$

$$\mathbf{D} = \begin{bmatrix} 1 & 0 & 1 & 0 \\ \frac{cn_1}{2L} & -\frac{ck_1}{L} & \frac{cn_1}{2L} & -\frac{ck_2}{L} \\ c_1 C & c_1 S & c_1 C_h & c_1 S_h \\ c_3\Phi_1 & c_3\Phi_2 & c_3\Phi_3 & c_3\Phi_4 \end{bmatrix} \tag{19}$$

where

$$\begin{aligned} c_1 &= (1-c)^{-\frac{n_1}{2}}, \quad c_3 = (1-c)^{-\frac{n_3}{2}} c/(2L) \\ n_1 &= n+1, \quad n_2 = n+2, \quad n_3 = n+3 \\ C_h &= \cosh\left(k_2\ln(1-c)\right), \quad S_h = \sinh\left(k_2\ln(1-c)\right) \\ C &= \cos\left(k_1\ln(1-c)\right), \quad S = \sin\left(k_1\ln(1-c)\right) \\ \Phi_1 &= n_1 C + 2k_1 S, \quad \Phi_2 = n_1 S - 2k_1 C \\ \Phi_3 &= n_1 C_h - 2k_2 S_h, \quad \Phi_4 = n_1 S_h - 2k_2 C_h \end{aligned} \tag{20}$$

and

$$\mathbf{F} = \begin{bmatrix} -E_1 n_1 \Lambda_1 & 2E_1 k_1 \Lambda_1 & E_1 n_1 \Lambda_2 & -2E_1 k_2 \Lambda_2 \\ E_2 \Lambda_3 & 4E_2 k_1 n_2 & -E_2 \Lambda_4 & 4E_2 k_2 n_2 \\ E_3 \Lambda_1 \Phi_1 & E_3 \Lambda_1 \Phi_2 & -E_3 \Lambda_2 \Phi_3 & -E_3 \Lambda_2 \Phi_4 \\ E_4(-\Lambda_3 C + 4k_1 n_2 S) & E_4(-\Lambda_3 S - 4k_1 n_2 C) & E_4(\Lambda_4 C_h - 4k_2 n_2 S_h) & E_4(\Lambda_4 S_h - 4k_2 n_2 C_h) \end{bmatrix} \tag{21}$$

where

$$\begin{aligned} E_1 &= EI_0 c^3/8L^3, \quad E_2 = EI_0 c^2/4L^2, \quad E_3 = E_1(1-c)^{\frac{n_1}{2}}, \quad E_4 = E_2(1-c)^{\frac{n_3}{2}} \\ \Lambda_1 &= 4k_1^2 + n_3^2, \quad \Lambda_2 = 4k_2^2 - n_3^2, \quad \Lambda_3 = 4k_1^2 - n_1 n_3, \quad \Lambda_4 = 4k_2^2 + n_1 n_3 \end{aligned} \tag{22}$$

By eliminating the unknown constant vector $\bar{\mathbf{c}}$ from Eqs. (17), the explicit expressions for the entries of the 4×4 dynamic stiffness matrix $\mathbf{K}$ of the non-uniform Bernoulli–Euler beam can be obtained

$$\mathbf{f} = \mathbf{F}\mathbf{D}^{-1}\mathbf{d} = \mathbf{K}\mathbf{d} \tag{23}$$

where

$$\mathbf{K} = \frac{EI_0}{\delta}\begin{bmatrix} K_{11} & K_{12} & K_{13} & K_{14} \\ & K_{22} & K_{23} & K_{24} \\ & & K_{33} & K_{34} \\ Symm. & & & K_{44} \end{bmatrix} \tag{24}$$

where explicit analytical expressions for the entries $K_{11} - K_{44}$ above for an individual element member can be deduced by using symbolic computation which are given in Appendix.

It should be noted in passing that δ in Eq. (A.11) is the common denominator of the dynamic stiffness matrix $\mathbf{K}$, which is a function of frequency ω. The roots ω_i from $\delta(\omega) = 0$ correspond to the natural frequencies of a fully clamped non-uniform beam.

Once the elemental dynamic stiffness matrices of Eq. (24) for each element are developed, they can be assembled directly to each other or to elements of other non-uniform or uniform beam elements. So that beam assemblies with uniform or other non-uniform beam members can be modelled.

3. The Wittrick-Williams algorithm and modal analysis

Each entry of the global dynamic stiffness matrix of the final structure obtained above is a transcendental function of frequency, and

the powerful solution technique of the Wittrick-Williams (WW) algorithm [41] will be applied to compute the natural frequencies. The WW algorithm uses the Sturm sequence property of the dynamic stiffness matrix to give the number of natural frequencies, below an arbitrarily chosen trial frequency $J(\omega^{\#})$. It is essentially a counting method. Its basic principles are briefly summarized as follows

$$J\left(\omega^{\#}\right) = J_0\left(\omega^{\#}\right) + s\left\{\mathbf{K}\left(\omega^{\#}\right)\right\} \tag{25}$$

where $\omega^{\#}$ is the trial frequency, $s\left\{\mathbf{K}(\omega^{\#})\right\}$ is the negative inertia index of the dynamic stiffness matrix under the trial frequency, which is essentially the number of negative diagonal terms in the upper triangular matrix that is formed from the dynamic stiffness matrix $\mathbf{K}(\omega^{\#})$ through the usual Gaussian elimination technique. $J_0(\omega^{\#})$ is the number of the natural frequencies lower than the trial frequency when all nodes of m elements of the structure are fully clamped, i.e. when $\mathbf{d} = \mathbf{0}$ in $\mathbf{Kd} = \mathbf{0}$. $J_0(\omega^{\#})$ can be determined by the following summation

$$J_0\left(\omega^{\#}\right) = \sum_{i=1}^{m} J_i\left(\omega^{\#}\right) \tag{26}$$

where $J_i(\omega^{\#})$ is the number of natural frequencies less than the trial frequency when all nodes of the ith element are fully clamped.

Based on the mode count given in Eq. (25), it is clear that as the trial frequency $\omega^{\#}$ passes a natural frequency, the value of integer $J(\omega^{\#})$ will increase by one. Following this procedure, any required natural frequencies can be computed to any required precision by using, say, the bisection method. As discussed in Section 1, the advantages of the WW algorithm include high efficiency, exact, reliable and analytical elegance. All of the four advantages are guaranteed under the precondition that the crucial issue of J_0 count to be resolved. Next we will give a discussion on three different solutions to the J_0 count problem

Solution 1 Discretize the structures into small enough elements such that $J_0 = 0$ always. However, more elements mean larger matrices, and therefore more expensive computation and lower efficiency. Therefore, it should be avoided as far as possible.

Solution 2 If the analytic solutions for mode count of a member with special boundary conditions (e.g., simple supports at both ends is J_s) which is somehow known, J_0 can be obtained by applying WW algorithm in the reverse direction, i.e., $J_0 = J_s - s(\mathbf{K}_s)$, where $\mathbf{K}_s$ is the DS of a simply supported beam, see [45] for example.

Solution 3 If the common denominator $\delta(\omega)$ of the DS matrix of the element has an analytical expression, then the J_0 can be derived from $\delta(\omega) = 0$, but this is only applicable to very simple uniform bars or beams. There are two situations that can arise for this case

(i) J_0 can be directly derived through the analysis of $\delta(\omega)$, such as the axial free vibration problem of the classical rod theory with constant section, see [41], which is not applicable to the case where J_0 cannot be derived from $\delta(\omega) = 0$, such as the tapered beam, considered here.

(ii) The J_0 expression cannot be obtained directly from the analytical expression of $\delta(\omega)$, so the $\delta(\omega)$ needs to be plotted, and the frequency that makes $\delta(\omega) = 0$ needs to be numerically found and saved. But this method can be error prone to miss natural frequencies, and it is time-consuming to determine the precise frequency that makes $\delta(\omega) = 0$.

As for tapered beam, the above Solution 1 works but is inefficient; Solution 2 is not applicable since analytical expression for the mode count of element with special boundary conditions (e.g., simply supported) cannot be easily deduced; Although the expression for the common denominator of the DS matrix is available, as given by Eq. (A.11), it is difficult to deduce J_0 directly from $\delta(\omega) = 0$ based on Eq. (A.11), so Solution (3i) is not suitable, while Solution (3ii) is inefficient and likely to miss some roots. Since all of the above method are not appropriate, therefore we propose a new method to provide an efficient and reliable method to compute J_0 with certainty for the DS element of a tapered beam.

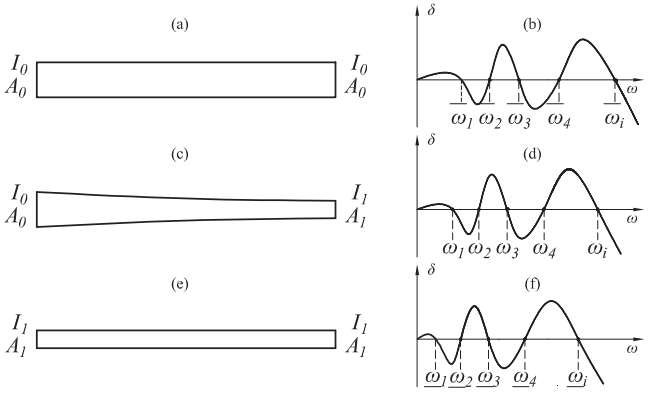

Fig. 3. The $\delta(\omega)$ plots shown in (b), (d) and (f) correspond to three cases, namely, (a) uniform beam with cross-section I_0, A_0, (c) tapered beam with cross-section I_0, A_0 and I_1, A_1 on both ends, and (e) uniform beam with cross-section I_1, A_1.

3.1. J_0 problem and natural frequencies

In this section, we make full use of the physical meaning and their properties of natural frequencies of a fully clamped element, namely, $\delta(\omega) = 0$, and propose an algorithm which computes J_0 that theoretically ensures high computational efficiency and also that no root can be missed. This method is not only very suitable for the non-uniform beam in this paper, but also can be extended to other DS elements that have $\delta(\omega)$ expressions but cannot derive the analytical expression for J_0.

First, we draw the $\delta(\omega)$ functions of three different beams, including a tapered beam and two uniform beams as examples, as shown in Fig. 3. To be more specific, the $\delta(\omega)$ plots shown in (b), (d) and (f) correspond respectively to the three cases, namely, (a) uniform beam with cross-section I_0, A_0, (c) tapered beam with cross-section I_0, A_0 and I_1, A_1 on two ends, and (e) uniform beam with cross-section I_1, A_1. We know that the common denominators of the DS matrices of two uniform Euler beams in Figs. (*a*) and (*e*) are already available, see e.g., [41].

$$\delta(\omega) = 1 - \cos\lambda \sin\lambda \tag{27}$$

where

$$\lambda = \left(\omega^2 L^4 \rho A / EI\right)^{1/4} \tag{28}$$

A close inspection on Fig. 3 reveals that

(1) For both uniform and non-uniform beams clamped at both ends, see Figs. 3 (b), (d) and (f), as the frequency ω increases from zero, the value of $\delta(\omega)$ starting from zero to positive first and then negative, followed by the curve changing from positive to negative values alternately.

(2) For the same order of natural frequencies for the three cases, larger cross-section leads to larger natural frequencies (i.e., $\underline{\omega_i} < \bar{\omega}_i$), and the tapered beam frequencies fall between the upper limit and the lower limit of the two, which is given by

$$\underline{\omega_i} < \omega_i < \bar{\omega}_i \tag{29}$$

The above rule is also physically explicable because larger stiffness means higher natural frequencies.

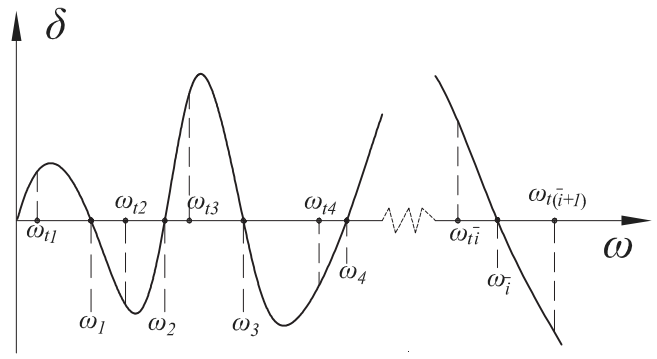

Fig. 4. The curve of $\delta(\omega)$ of the DS matrix of a non-uniform beam versus frequency.

Table 2
The sign of δ and J_0 versus frequency ω_{ti} for a fully clamped non-uniform beam.

Frequencies	ω_{t1}	ω_{t2}	ω_{t3}	ω_{t4}	...	ω_{ti}	...
sign($\delta(\omega_{ti})$)	1	−1	1	−1	...	1 or −1	...
$J_0(\omega_{ti})$	0	1	2	3	...	*i*-1	...

(3) The difference between two adjacent natural frequencies of uniform beams and non-uniform beams is not a constant. Let $(\Delta\omega)_i = \omega_{i+1} - \omega_i$, $(\overline{\Delta\omega})_i = \bar{\omega}_{i+1} - \bar{\omega}_i$, $(\underline{\Delta\omega})_i = \underline{\omega}_{i+1} - \underline{\omega}_i$, three of which increase with the cross-section size and frequency range; and the difference between the two adjacent natural frequencies $(\Delta\omega)_i$ of a fully clamped tapered beam lies between that of the two uniform beams, which is

$$(\underline{\Delta\omega})_i < (\Delta\omega)_i < (\overline{\Delta\omega})_i \tag{30}$$

We are now in position to evaluate $\delta(\omega_{ti})$ and $J_0(\omega_{ti})$ at certain values of ω as shown in Fig. 4. However, in order to ensure that no roots will be missed and meanwhile the computational cost is reduced to the minimum, it is necessary to take appropriate values of the initial value and the step-size of frequencies where $\delta(\omega)$ is to be evaluated. According to the above observations, we may take $\underline{\omega}_1$ as the initial frequency, and $(\underline{\Delta\omega})_1$ as the step-size to evaluate $\delta(\omega)$, with different positive or negative signs, see Fig. 4. If the signs of $\delta(\omega)$ of two or more adjacent frequencies are the same, we keep any one of them and discard the rest, resulting in an ascending list of $\omega_{ti}(i = 1, 2, 3...)$ with alternative positive and negative signs. Meanwhile, the sign count $J_0(\omega_{ti})$ can be determined and recorded, as shown in Table 2. By doing so, the roots of $\delta(\omega) = 0$, i.e. $\omega_i(i = 1, 2, 3, \ldots)$ (where J_0 shifts) will be located between two adjacent ω_{ti}'s in the list and then $J_0(\omega_{ti})$ can be determined, as clearly illustrated in Fig. 4.

It is now straightforward to determine $J_0(\omega^{\#})$ at a given $\omega^{\#}$ based on Table 2. We first find a pair of adjacent $(\omega_{tj}, \omega_{t(j+1)})$ such that $\omega_{tj} < \omega^{\#} < \omega_{t(j+1)}$. Then we evaluate sign($\delta(\omega^{\#})$) which must lead to either sign($\delta(\omega^{\#})$) = sign($\delta(\omega_{tj})$) or sign($\delta(\omega^{\#})$) = sign($\delta(\omega_{t(j+1)})$). If the former equation holds, it means that there is no natural frequency between $\omega^{\#}$ and ω_{tj}, therefore $J_0(\omega^{\#}) = J_0(\omega_{tj}) = j - 1$. If the latter holds, $J_0(\omega^{\#}) = J_0(\omega_{t(j+1)}) = j$. The above procedure has been written as a flow chart shown in Fig. 5. The idea of this highly efficient and exact algorithm can also be applied to other non-uniform elements, such as functionally graded beams.

In summary, we first make use of the upper and lower limits of uniform beams of both eigen-frequencies and their differences between two adjacent eigenvalues of a fully clamped tapered beams. Then, we evaluation the analytical function of $\delta(\omega)$ at the appropriate pre-determined frequencies and create ascending table of $\delta(\omega)$ with alternatingly positive and negative values. Finally, the J_0 at any trial frequency is obtained by comparing the trial frequency and the ascending table of $\delta(\omega)$, together with comparison on the sign of $\delta(\omega^{\#})$ and that of ascending table $\delta(\omega)$. In this way, no root of $\delta(\omega) = 0$ is missed, and at the same time, the computation efficiency is improved very considerably.

3.2. Modal shape computation

After the natural frequencies are computed, one can recover the mode shapes in a straightforward manner. By letting an entry of the displacement vector corresponding to an appropriate degree of freedom equal to 1, the displacement vector in the global coordinate system can be obtained. Then the displacement vector of each element in the local coordinate system can be obtained by applying the transformation matrix. The unknown coefficient vector $\bar{\mathbf{c}}$ can be obtained from $\bar{\mathbf{c}} = \mathbf{D}^{-1}\mathbf{d}$ by recalling Eq. (17). Finally, the mode shapes corresponding to the natural frequency can be recovered.

4. Results and discussions

The method described in this paper has been implemented in a MATLAB program to calculate the natural frequencies and mode shapes of non-uniform beams and their assemblies. First, Section 4.1 illustrates the high efficiency and exactness of the current method by comparing it with the FEM. Section 4.2 validates the present results with the existing results under different taper/functional gradient rates c. In Section 4.3, we explore the effect of the taper/functional gradient index n on the natural frequencies. Then, in Section 4.4, we compute the natural frequencies of the tapered beam under all possible 16 boundary conditions. Finally, Section 4.5 shows the application of the proposed method to the modal analysis of a beam assembly consisting of two parabolically tapered beams.

It should be noted that the letters 'C', 'G', 'P' and 'F' in this paper represent 'clamped', 'guided', 'pinned' and 'free' boundary conditions, respectively. The letters on the left represent boundary condition on the larger cross-section, and the letters on the right represent boundary condition on the smaller cross-section. 'BCs' is, of course, an abbreviation for boundary conditions and 'NOE' is an abbreviation for the number of elements. All results obtained by the present method are exact solutions without any approximation, and all are accurate to the last digit, specified and result can be obtained up to machine accuracy if needed.

4.1. Efficiency and exactness

All the beams in numerical examples are made of steel (elasticity modulus $E_0 = 2.0 \times 10^{11}\text{N/m}^2$, density $\rho_0 = 7850\text{kg/m}^3$). Here we consider a tapered beam with annular section of length $l = 25\text{m}$, taper/functional gradient rate $c = 0.7$, taper/functional gradient index $n = 4$, outer radius $R_{a0} = 0.1\text{m}$ and inner radius $r_{a0} = 0.05\text{m}$. Table 3 shows the first eight natural frequencies subject to three BCs computed by the present method and compared with those computed by FE software ANSYS. Side by side the number of elements and total computational time are also shown. All the computations in this paper are performed on the same computer with an Intel core i5-9400 CPU with 8 GB RAM. In ANSYS software, we used 100, 200, 600, 900 elements to simulate the beam, taking at least 0.16s, 0.9s, 1.0s, 1.1s, respectively. With the increase of the number of elements, the results of FEM gradually tend to the results of the analytical method.(When the tapered beam is analysed by FEM with different number of elements, the convergence rate is much slower than that of uniform cross-section beams, as expected.) By contrast, the present method only needs one element to compute the first eight exact natural frequencies, taking maximum 0.018s, about less than 1% of the time used by the FEM. This is a very low degree of freedom and yet, gives very high computational efficiency. Compared with FEM, the method presented in this paper has clear advantages in modal analysis of tapered and/or functionally graded beam.

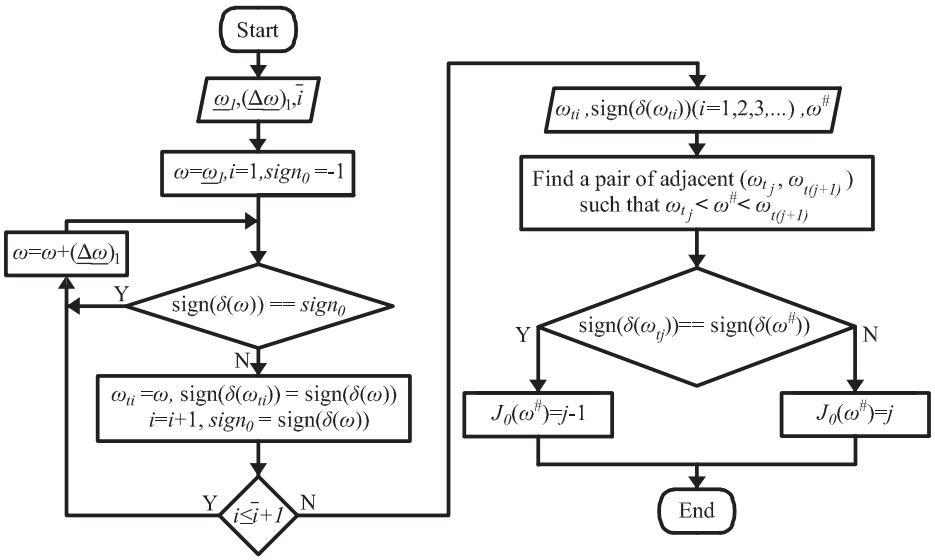

Fig. 5. The flow chart for computing the J_0 count of a tapered beam. The 'sign' is the sign function and '==' is the equal operator. $\bar{i}$ is the maximum order of the natural frequency to be solved.

Table 3
Comparison of NOE used and computational time for computing the first eight natural frequencies of a parabolically tapered beam by using present method and the FEM package (ANSYS).

BCs	NOE	Time(s)	Natural frequencies (Hz)							
C-F			1	2	3	4	5	6	7	8
Present	1	0.018	0.49243	1.0687	2.0769	3.5420	5.4760	7.8837	10.768	14.129
	100	0.1719	0.49031	1.0732	2.1006	3.6084	5.5691	8.0278	10.972	14.428
FEM	200	0.959	0.49165	1.0690	2.0799	3.5498	5.4912	7.9113	10.816	14.196
	600	1.039	0.49191	1.0684	2.0772	3.5432	5.4779	7.8863	10.770	14.131
	900	1.229	0.49191	1.0684	2.0771	3.5431	5.4777	7.8858	10.769	14.130
C-P			1	2	3	4	5	6	7	8
Present	1	0.016	0.69737	1.5906	2.9412	4.7588	7.0493	9.8153	13.058	16.779
	100	0.1694	0.70155	1.6087	2.9765	4.8054	7.1670	9.9783	13.303	17.142
FEM	200	0.983	0.69788	1.5936	2.9485	4.7732	7.0741	9.8516	13.102	16.843
	600	1.051	0.69731	1.5911	2.9424	4.7609	7.0521	9.8187	13.062	16.782
	900	1.124	0.69731	1.5911	2.9423	4.7607	7.0517	9.8178	13.060	16.779
C-C			1	2	3	4	5	6	7	8
Present	1	0.016	0.76292	1.7503	3.2065	5.1355	7.5403	10.422	13.783	17.621
	100	0.1673	0.76606	1.7659	3.2452	5.1833	7.6507	10.590	14.045	18.002
FEM	200	0.925	0.76349	1.7528	3.2124	5.1473	7.5624	10.460	13.833	17.682
	600	1.011	0.76291	1.7507	3.2073	5.1364	7.5409	10.422	13.781	17.618
	900	1.103	0.76290	1.7506	3.2071	5.1361	7.5403	10.421	13.779	17.615

4.2. Validation and dependence of natural frequencies on taper/functional gradient rate c

In this section, we consider tapered beams and functionally graded beams with annular cross-section sharing the same bending stiffness and linear density of length $l = 2$m, different taper/functional gradient rates c including 0, 0.1, 0.3, 0.5, 0.7, and 0.8, taper/functional gradient index $n = 4$, outer radius $R_{a0} = 0.1$m and inner radius $r_{a0} = 0.05$m. Thus the linear density is $\rho(x)A(x) = \rho_0 A_0 (1 - cx/L)^4$ and the bending stiffness is $E(x)I(x) = E_0 I_0 (1 - cx/L)^8$. Results show the natural frequencies of the two beams that share the same bending stiffness and linear density are equal. Table 4 compares the results of the tapered (or functionally graded) beam subject to C-F BC computed by the present method with those by the Galerkin method [20]. All the present results are accurate up to the last digits. It can be observed that the results of both methods agree very well. It is seen that under the C-F BC condition, the fundamental natural frequency increases with the increase of c, while the remaining natural frequencies decrease with the increase of c. Similar observation was made in [20].

Table 4
Comparisons of natural frequencies of C-F tapered (or functionally graded) beams with different taper/functional gradient rates c by using the present method and the Galerkin method [20].

Modes	Methods	Natural frequencies (Hz)					
		$c = 0$	$c = 0.1$	$c = 0.3$	$c = 0.5$	$c = 0.7$	$c = 0.8$
1	Galerkin [20]	39	43	52	62	77	85
	Present	39.474	43.003	51.563	62.656	76.943	85.393
2	Galerkin [20]	247	236	214	191	167	154
	Present	247.38	236.49	214.06	190.93	166.98	154.16
3	Galerkin [20]	693	637	530	427	325	272
	Present	692.68	637.46	530.37	426.82	324.51	271.87

4.3. Dependence of natural frequencies on taper/functional gradient index n

In this section, we consider tapered beams and functionally graded beams with two different cross-section types sharing the same bending stiffness and linear density. The beam is of length $l = 2$m, taper/functional gradient rate $c = 0.1$, different taper/functional gradient

Table 5
The first eight natural frequencies of tapered (or functionally graded) beam with different taper/functional gradient indexes n with rectangular or annular cross-section.

Cross section	n	Natural frequencies (Hz)							
		1	2	3	4	5	6	7	8
Rectangular	−2	0.11750	0.73656	2.0623	4.0412	6.6804	9.9794	13.938	18.557
	0	0.12529	0.75130	2.0766	4.0556	6.6948	9.9938	13.953	18.571
	1/3	0.12663	0.75379	2.0791	4.0581	6.6973	9.9962	13.955	18.574
	2	0.13350	0.76631	2.0915	4.0706	6.7098	10.009	13.968	18.586
	4	0.14212	0.78160	2.1068	4.0861	6.7255	10.025	13.983	18.602
Annular	4	0.27522	1.5136	4.0798	7.9128	13.024	19.412	27.079	36.022

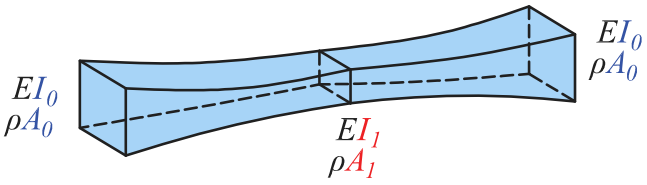

Fig. 6. A parabolically tapered beam assembly.

indexes n taking −2, 0, 1/3, 2, and 4, outer radius $R_{a0} = 0.1$m and inner radius $r_{a0} = 0.05$m for the ones with annular section, and width $b_0 = 0.1$m and height $h_0 = 0.1$m for those with rectangular section. Therefore the linear density is $\rho(x)A(x) = \rho_0 A_0 (1 - 0.1x/L)^n$ and the bending stiffness is $E(x)I(x) = E_0 I_0 (1 - 0.1x/L)^{n+4}$. Results show the natural frequencies of the tapered beams and the functionally graded beams that share the same bending stiffness and linear density are equal. Table 5 tabulates the first eight natural frequencies of parabolically tapered (or functionally graded) beams with several types of cross sections identified by different taper/functional gradient indexes n. The BCs are taken to be C-F. The results show that as the taper/functional gradient index n increases, which means the sharper the beam, the higher the natural frequency.

4.4. Effects of different boundary conditions

Next, we will demonstrate that this method is easy to model beams subject to different BCs. It is possible that a tapered beam can have 16 different combinations of BCs (see Table 6) whereas a uniform beam can only have 10 different combinations. Table 6 shows the first eight natural frequencies of a parabolically tapered beam with all 16 BCs. The parameters of the beam are the same as those in Table 3. It can be seen that the non-rigid body natural frequencies of F-F and C–C BCs are identical; Also, the natural frequencies of P-F and C-P BCs, F-P and P-C BCs beams have the same non-rigid bodies natural frequencies. This finding is consistent with that of uniform beams.

4.5. Beam assembly consisting of two parabolically tapered beam elements

The dynamic stiffness (DS) elements of tapered and functionally graded beam proposed in this paper can be assembled directly with the DS those of available tapered elements and/or those with uniform cross sections. Here, the presented method is used to model a beam assembly, which is composed of two parabolically tapered beams, as shown in Fig. 6. All data of the two parabolically tapered beams are the same as those in Section 4.1 except that the two beams have different lengths, which are 10m and 15m respectively. Modal analysis of the beam is carried out under three typical BCs, namely C–C, P-P, and C-F. The letters on the left represent the BC on the left end of the beam assembly, and the letters on the right represent the BC on the right. 500 elements are used to determine first eight natural frequencies and it takes 2.3s, while the proposed method use only 2 elements and costs only 0.02s which is 100 times faster. The natural frequencies and corresponding mode shapes calculated by the proposed method and ANSYS software shown in Fig. 7. All results have five significant digit precision and they agree with each other very well. It is easily seen from the fundamental mode shapes that the free vibration waves are localized in the centre section where bending stiffnesses are smaller, which is in a sharp contract to those of a uniform beam, as expected.

5. Conclusions

Closed-form dynamic stiffness (DS) formulation for tapered/functionally graded beams has been proposed. The formulation is based on the exact general solution of the governing differential equation of a non-uniform Euler–Bernoulli beam, and explicit expressions are derived. The developed DS is applicable to a wide range of tapered and/or functionally graded beams whose bending stiffness and linear density are assumed to be polynomial functions of position. This is significant in the context that existing research is predominantly confined to linearly tapered/functionally graded beams only. As a well-established solution technique, the Wittrick-Williams algorithm is applied for exact modal analysis of individual tapered beam as well as their assemblies. The most crucial issue, the J_0 count of the WW algorithm is resolved in an elegant and efficient manner. The two novelties in both the DS formulation and the solution technique make exact and highly efficient modal analysis possible for any combinations of tapered profiles, without resorting to series solution, numerical integrations or refined mesh discretization. Benchmark solutions have been provided for tapered and functionally graded beams with different taper/functional gradient rates, taper/functional gradient indexes and boundary conditions. The proposed research provides a necessary and significant supplement to the existing closed-form DS element library of beams, which can be used in parametric studies and optimal design of beam assemblies with tapered/functionally graded members. The limitation of this paper is that the Euler–Bernoulli beam theory is only applicable to beams with high slenderness, which can be broken through by developing the dynamic stiffness formulations for tapered beams based on Timoshenko theory.

CRediT authorship contribution statement

Xiang Liu: Conceptualization, Methodology, Writing – review & editing, Supervision, Project administration, Funding acquisition. **Le Chang:** Investigation, Data curation, Writing – original draft, Writing – review & editing. **J. Ranjan Banerjee:** Supervision, Writing – review & editing. **Han-Cheng Dan:** Writing – review & editing.

Declaration of competing interest

The authors declare that they have no known competing financial interests or personal relationships that could have appeared to influence the work reported in this paper.

Table 6
The first eight natural frequencies for a parabolically tapered beam subject to 16 different combinations of end constrains.

BCs	Natural frequencies (Hz)							
	1	2	3	4	5	6	7	8
F-F	0	0	0.76292	1.7503	3.2065	5.1355	7.5403	10.422
F-G	0	0.022486	0.82142	1.9056	3.4692	5.5108	8.0307	11.029
F-P	0	0.18687	1.2402	2.5940	4.4115	6.7014	9.4668	12.709
F-C	0.0060803	0.23785	1.3881	2.8520	4.7833	7.1889	10.071	13.432
G-F	0	0.53219	1.1878	2.2932	3.8655	5.9114	8.4338	11.434
G-G	0	0.55544	1.2802	2.4809	4.1599	6.3178	8.9550	12.072
G-P	0.041063	0.78472	1.7772	3.2347	5.1643	7.5694	10.452	13.812
G-C	0.054572	0.86510	1.9577	3.5242	5.5670	8.0876	11.087	14.565
P-F	0	0.69737	1.5906	2.9412	4.7588	7.0493	9.8153	13.058
P-G	0.014380	0.74524	1.7273	3.1811	5.1090	7.5131	10.395	13.755
P-P	0.14626	1.1118	2.3593	4.0652	6.2406	8.8899	12.015	15.618
P-C	0.18687	1.2402	2.5940	4.4115	6.7014	9.4668	12.709	16.430
C-F	0.49243	1.0687	2.0769	3.5420	5.4760	7.8837	10.768	14.129
C-G	0.50991	1.1466	2.2441	3.8127	5.8567	8.3780	11.378	14.856
C-P	0.69737	1.5906	2.9412	4.7588	7.0493	9.8153	13.058	16.779
C-C	0.76292	1.7503	3.2065	5.1355	7.5403	10.422	13.783	17.621

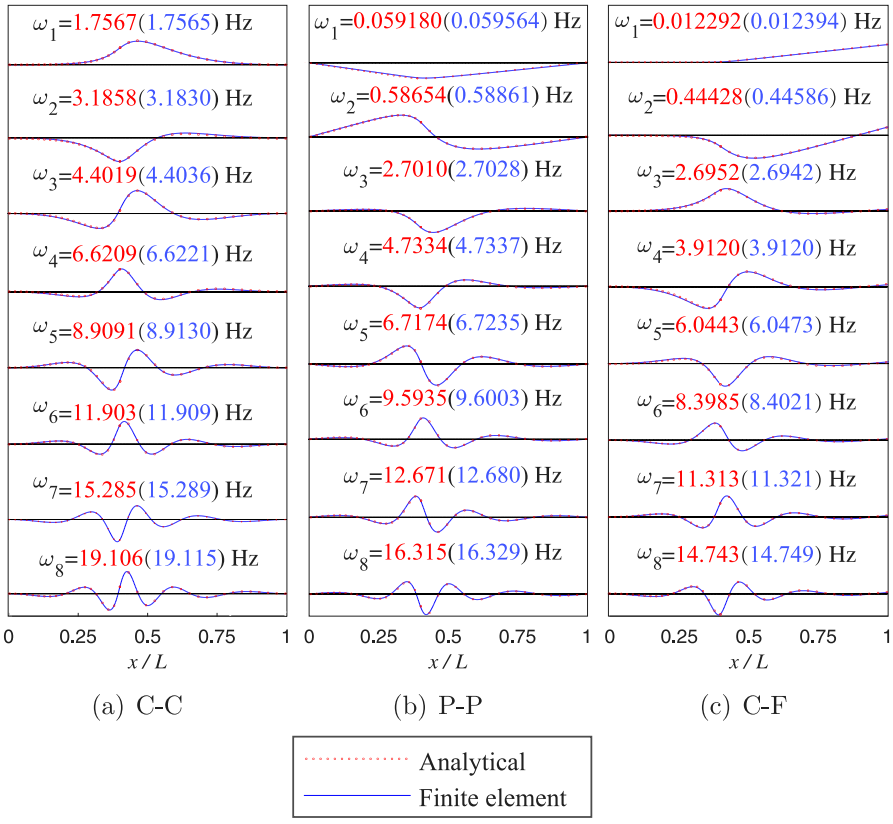

Fig. 7. The first eight natural frequencies and mode shapes for the beam shown in Fig. 6 subject to 3 sets of classical BCs calculated by two methods.

Acknowledgements

The authors appreciate the supports from National Natural Science Foundation (Grant No. 11802345), State Key Laboratory of High Performance Complex Manufacturing, China (Grant No. ZZYJKT2019-07), Central South University (Grant No. 502045001) which made this research possible. The authors are grateful to the discussions on general solutions with X.W. Zhao from University of Shanghai for Science and Technology.

Appendix

The explicit expressions for each entries $K_{11} - K_{44}$ of the dynamic stiffness matrix of Eq. (24) of the tapered/functionally graded beam element are given as,

$$K_{11} = -c^3 P_1 \left(C_h k_2 \left(4k_1^2 + n_1^2\right) S + S_h \left(Ck_1 \left(4k_2^2 - n_1^2\right) + 2P_1 n_1 S\right)\right)/(4L^3) \tag{A.1}$$

$$K_{12} = c^2 \left(4k_1 k_2 n_2 - 2C_h k_2 (2Ck_1 n_2 + P_1 n_1 S) + S_h (2Ck_1 P_1 n_1 + (-k_2^2 n_1^2 + k_1^2(-8k_2^2 + n_1^2))S)\right)/(4L^2) \tag{A.2}$$

$$K_{13} = (1-c)^{\frac{n_1}{2}} c^3 P_1 \left(k_1 \left(4k_2^2 - n_1^2\right) S_h + k_2 \left(4k_1^2 + n_1^2\right) S\right)/(4L^3) \tag{A.3}$$

$$K_{14} = -(1-c)^{\frac{n_3}{2}} c^2 P_1 (-2C_h k_1 k_2 + 2Ck_1 k_2 - k_1 n_1 S_h + k_2 n_1 S)/(2L^2) \tag{A.4}$$

$$K_{22} = c\left(-2k_1 k_2 n_2 - C_h k_2 \left(-2Ck_1 n_2 + P_1 S\right) + S_h \left(Ck_1 P_1 + P_2 n_2 S\right)\right)/L$$

(A.5)

$$K_{23} = (1-c)^{\frac{n_1}{2}} c^2 P_1(-2C_h k_1 k_2 + 2Ck_1 k_2 + k_1 n_1 S_h - k_2 n_1 S)/(2L^2) \quad \text{(A.6)}$$

$$K_{24} = -(1-c)^{\frac{n_3}{2}} c P_1(k_1 S_h - k_2 S)/L \quad \text{(A.7)}$$

$$K_{33} = -(1-c)^{n_1} c^3 P_1 \left(C_h k_2 \left(4k_1^2 + n_1^2\right) S - S_h \left(Ck_1 \left(-4k_2^2 + n_1^2\right) + 2P_1 n_1 S\right)\right)/(4L^3) \quad \text{(A.8)}$$

$$K_{34} = -(1-c)^{n_2} c^2 \left(-4k_1 k_2 n_2 - 2Chk_2(-2Ck_1 n_2 + (k_1^2 + k_2^2) n_1 S) + S_h(2Ck_1 P_1 n_1 + (k_2^2 n_1^2 + k_1^2(8k_2^2 - n_1^2))S)\right)/(4L^2) \quad \text{(A.9)}$$

$$K_{44} = (1-c)^{n_3} c \left(2k_1 k_2 n_2 - C_h k_2 \left(2Ck_1 n_2 + P_1 S\right) + S_h \left(Ck_1 P_1 - P_2 n_2 S\right)\right)/L \quad \text{(A.10)}$$

$$\delta = 2k_1 k_2 - 2C_h Ck_1 k_2 - P_2 S_h S \quad \text{(A.11)}$$

where

$$P_1 = k_1^2 + k_2^2, \quad P_2 = k_1^2 - k_2^2 \quad \text{(A.12)}$$

and the notations such as c, n_1, P_1, P_2, S, C, S_h, C_h, etc. have been defined in Eqs. (1)–(22).

References

[1] Krylov V, Winward R. Experimental investigation of the acoustic black hole effect for flexural waves in tapered plates. J Sound Vib 2007;300(1–2):43–9. http://dx.doi.org/10.1016/j.jsv.2006.07.035.

[2] Kalkowski MK, Muggleton JM, Rustighi E. An experimental approach for the determination of axial and flexural wavenumbers in circular exponentially tapered bars. J Sound Vib 2017;390:67–85. http://dx.doi.org/10.1016/j.jsv.2016.10.018.

[3] Erturk A, Inman D. A distributed parameter electromechanical model for cantilevered piezoelectric energy harvesters. J Vib Acoust Trans ASME 2008;130(4):1–15. http://dx.doi.org/10.1115/1.2890402.

[4] Shahba A, Attarnejad R, Hajilar S. Free vibration and stability of axially functionally graded tapered Euler-Bernoulli beams. Shock Vib 2011;18(5):683–96. http://dx.doi.org/10.3233/SAV-2010-0589.

[5] Shahba A, Attarnejad R, Marvi MT, Hajilar S. Free vibration and stability analysis of axially functionally graded tapered Timoshenko beams with classical and non-classical boundary conditions. Composites B 2011;42(4):801–8. http://dx.doi.org/10.1016/j.compositesb.2011.01.017.

[6] Vinod K, Gopalakrishnan S, Ganguli R. Free vibration and wave propagation analysis of uniform and tapered rotating beams using spectrally formulated finite elements. Int J Solids Struct 2007;44(18–19):5875–93. http://dx.doi.org/10.1016/j.ijsolstr.2007.02.002.

[7] Ramalingerswara Rao S, Ganesan N. Dynamic response of tapered composite beams using higher order shear deformation theory. J Sound Vib 1995;187(5):737–56. http://dx.doi.org/10.1006/jsvi.1995.0560.

[8] Abrate S. Vibration of non-uniform rods and beams. J Sound Vib 1995;185(4):703–16. http://dx.doi.org/10.1006/jsvi.1995.0410.

[9] Zhou D, Cheung Y. Free vibration of a type of tapered beams. Comput Methods Appl Mech Engrg 2000;188(1):203–16. http://dx.doi.org/10.1016/S0045-7825(99)00148-6.

[10] Cheung Y, Zhou D. Vibration of tapered Mindlin plates in terms of static Timoshenko beam functions. J Sound Vib 2003;260(4):693–709. http://dx.doi.org/10.1016/S0022-460X(02)01008-8.

[11] El-Sayed T, El-Mongy H. Application of variational iteration method to free vibration analysis of a tapered beam mounted on two-degree of freedom subsystems. Appl Math Model 2018;58:349–64. http://dx.doi.org/10.1016/j.apm.2018.02.005.

[12] Huang Y, Li XF. A new approach for free vibration of axially functionally graded beams with non-uniform cross-section. J Sound Vib 2010;329(11):2291–303. http://dx.doi.org/10.1016/j.jsv.2009.12.029.

[13] Ashour A. A semi-analytical solution of the flexural vibration of orthotropic plates of variable thickness. J Sound Vib 2001;240(3):431–45. http://dx.doi.org/10.1006/jsvi.2000.3238.

[14] Cao D, Gao Y, Yao M, Zhang W. Free vibration of axially functionally graded beams using the asymptotic development method. Eng Struct 2018;173(June):442–8. http://dx.doi.org/10.1016/j.engstruct.2018.06.111.

[15] Hein H, Feklistova L. Free vibrations of non-uniform and axially functionally graded beams using haar wavelets. Eng Struct 2011;33(12):3696–701. http://dx.doi.org/10.1016/j.engstruct.2011.08.006.

[16] Banerjee J, Ananthapuvirajah A, Papkov S. Dynamic stiffness matrix of a conical bar using the Rayleigh-Love theory with applications. Eur J Mech, A/Solids 2020;83(April):104020. http://dx.doi.org/10.1016/j.euromechsol.2020.104020.

[17] Mahmoud M. Natural frequency of axially functionally graded, tapered cantilever beams with tip masses. Eng Struct 2019;187(December 2018):34–42. http://dx.doi.org/10.1016/j.engstruct.2019.02.043.

[18] Ece MC, Aydogdu M, Taskin V. Vibration of a variable cross-section beam. Mech Res Commun 2007;34(1):78–84. http://dx.doi.org/10.1016/j.mechrescom.2006.06.005.

[19] Wu J-S. Analytical solutions for non-uniform continuous systems: tapered beams. In: Analytical and numerical methods for vibration analyses. Singapore: John Wiley & Sons; 2013, p. 173–243.

[20] Zhao XW, Hu ZD, van der Heijden GH. Dynamic analysis of a tapered cantilever beam under a travelling mass. Meccanica 2015;50(6):1419–29. http://dx.doi.org/10.1007/s11012-015-0112-5.

[21] Rajesh K, Saheb K. Large amplitude free vibration analysis of tapered Timoshenko beams using coupled displacement field method. Int J Appl Mech Eng 2018;23(3):673–88. http://dx.doi.org/10.2478/ijame-2018-0037.

[22] Banerjee J, Ananthapuvirajah A. Free flexural vibration of tapered beams. Comput Struct 2019;224:106106. http://dx.doi.org/10.1016/j.compstruc.2019.106106.

[23] Koloušek V. Anwendung des Gesetzes der virtuellen Verschiebungen und des Reziprozitätssatzes in der Stabwerksdynamik. Ing-Arch 1941;12(6):363–70. http://dx.doi.org/10.1007/BF02089894.

[24] Wittrick W, Williams F. A general algorithm for computing natural frequencies of elastic structures. Q J Mech Appl Math 1970;XXIV:263–84. http://dx.doi.org/10.1093/qjmam/24.3.263.

[25] Williams F, Banerjee J. Flexural vibration of axially loaded beams with linear or parabolic taper. J Sound Vib 1985;99(1):121–38. http://dx.doi.org/10.1016/0022-460X(85)90449-3.

[26] Banerjee J, Williams F. Further flexural vibration curves for axially loaded beams with linear or parabolic taper. J Sound Vib 1985;102(3):315–27. http://dx.doi.org/10.1016/S0022-460X(85)80145-0.

[27] Anderson M, Williams F. BUNVIS-RG: An exact buckling and vibration program for lattice structures, with repetitive geometry and substructuring options. In: Collection of technical papers - AIAA/ASME/ASCE/AHS/ASC structures, structural dynamics and materials conference. (pt 2):1986, p. 211–20. http://dx.doi.org/10.2514/6.1986-868.

[28] Banerjee J. Free vibration of centrifugally stiffened uniform and tapered beams using the dynamic stiffness method. J Sound Vib 2000;233(5):857–75. http://dx.doi.org/10.1006/jsvi.1999.2855.

[29] Yuan S, Ye K, Xiao C, Williams F, Kennedy D. Exact dynamic stiffness method for non-uniform Timoshenko beam vibrations and Bernoulli-Euler column buckling. J Sound Vib 2007;303(3–5):526–37. http://dx.doi.org/10.1016/j.jsv.2007.01.036.

[30] Banerjee J, Su H, Jackson D. Free vibration of rotating tapered beams using the dynamic stiffness method. J Sound Vib 2006;298(4–5):1034–54. http://dx.doi.org/10.1016/j.jsv.2006.06.040.

[31] Banerjee J, Jackson D. Free vibration of a rotating tapered Rayleigh beam: A dynamic stiffness method of solution. Comput Struct 2013;124:11–20. http://dx.doi.org/10.1016/j.compstruc.2012.11.010.

[32] Leung A, Zhou W. Dynamic stiffness analysis of non-uniform Timoshenko beams. J Sound Vib 1995;181(3):447–56. http://dx.doi.org/10.1006/jsvi.1995.0151.

[33] Lee JW, Lee JY. Free vibration analysis of functionally graded Bernoulli-Euler beams using an exact transfer matrix expression. Int J Mech Sci 2017;122(December 2016):1–17. http://dx.doi.org/10.1016/j.ijmecsci.2017.01.011.

[34] Kim T, Lee B, Lee U. State-vector equation method for the frequency domain spectral element modeling of non-uniform one-dimensional structures. Int J Mech Sci 2019;157–158(April):75–86. http://dx.doi.org/10.1016/j.ijmecsci.2019.04.030.

[35] Banerjee J, Williams F. Exact Bernoulli-Euler dynamic stiffness matrix for a range of tapered beams. Internat J Numer Methods Engrg 1985;21:2289–302. http://dx.doi.org/10.1002/nme.1620211212.

[36] Su H, Banerjee J, Cheung C. Dynamic stiffness formulation and free vibration analysis of functionally graded beams. Compos Struct 2013;106:854–62. http://dx.doi.org/10.1016/j.compstruct.2013.06.029.

[37] Banerjee J, Ananthapuvirajah A. Free vibration of functionally graded beams and frameworks using the dynamic stiffness method. J Sound Vib 2018;422:34–47. http://dx.doi.org/10.1016/j.jsv.2018.02.010.

[38] Popov A. Comments on "Free vibration of functionally graded beams and frameworks using the dynamic stiffness method [J. Sound Vib. 422(2018) 34–47]". J Sound Vib 2020;466:115007. http://dx.doi.org/10.1016/j.jsv.2019.115007.

[39] Banerjee J. Review of the dynamic stiffness method for free-vibration analysis of beams. Transp Saf Environ 2019;1(2):106–16. http://dx.doi.org/10.1093/tse/tdz005.

[40] Han H, Liu L, Cao D. Analytical approach to coupled bending-torsional vibrations of cracked Timoshenko beam. Int J Mech Sci 2020;166:105235. http://dx.doi.org/10.1016/j.ijmecsci.2019.105235.

[41] Williams F, Wittrick W. A automatic computational procedure for calculating natural frequencies of skeletal structures. Int J Mech Sci 1970;12:781–91. http://dx.doi.org/10.1016/0020-7403(70)90053-6.

[42] Kumar S, Jana P. Application of dynamic stiffness method for accurate free vibration analysis of sigmoid and exponential functionally graded rectangular plates. Int J Mech Sci 2019;163(August):105105. http://dx.doi.org/10.1016/j.ijmecsci.2019.105105.

[43] Wittrick W, Williams F. An algorithm for computing critical buckling loads of elastic structures. J Struct Mech 1973;1(4):497–518. http://dx.doi.org/10.1080/03601217308905354.

[44] Williams F. A pocket calculator program for some simple vibration problems. Comput Struct 1978;9(4):427–9.

[45] Howson W, Williams F. Natural frequencies of frames with axially loaded Timoshenko Members. J Sound Vib 1973;26(4):503–15. http://dx.doi.org/10.1016/S0022-460X(73)80216-0.

[46] Howson W, Banerjee J, Williams F. Concise equations and program for exact eigensolutions of plane frames including member shear. In: Adey R, editor. Engineering Software III. Berlin, Heidelberg: Springer; 1983, p. 443–52. http://dx.doi.org/10.1007/978-3-662-02335-8_35.

[47] Banerjee J, Williams F. An exact dynamic stiffness matrix for coupled extensional-torsional vibration of structural members. Comput Struct 1994;50(2):161–6. http://dx.doi.org/10.1016/0045-7949(94)90292-5.

[48] Ghandi E, Rafezy B, Howson W. On the bi-planar motion of a Timoshenko beam with shear resistant in-fill. Int J Mech Sci 2012;57(1):1–8. http://dx.doi.org/10.1016/j.ijmecsci.2011.12.011.

[49] Banerjee J, Ananthapuvirajah A. An exact dynamic stiffness matrix for a beam incorporating Rayleigh–Love and Timoshenko theories. Int J Mech Sci 2019;150(October 2018):337–47. http://dx.doi.org/10.1016/j.ijmecsci.2018.10.012.

[50] Liu X, Liu X, Xie S. A highly accurate analytical spectral flexibility formulation for buckling and wrinkling of orthotropic rectangular plates. Int J Mech Sci 2020;168(March):105311. http://dx.doi.org/10.1016/j.ijmecsci.2019.105311.